

High-order, Dispersionless, Spatio-Temporally Parallel “Fast-Hybrid” Wave Equation Solver at $\mathcal{O}(1)$ Sampling Cost

Thomas G. Anderson^{1*}, Oscar P. Bruno¹, and Mark Lyon²

(Preliminary Draft)

¹ Computing & Mathematical Sciences, California Institute of Technology

² Department of Mathematics & Statistics, University of New Hampshire

Abstract

This paper proposes a frequency/time hybrid integral-equation method for the time dependent wave equation in two and three-dimensional spatial domains. Relying on Fourier Transformation in time, the method utilizes a fixed (time-independent) number of frequency-domain integral equation solutions to evaluate, with superalgebraically-small errors, time domain solutions for arbitrarily long times. The approach relies on two main elements, namely, 1) A smooth time-windowing methodology that enables smooth time partitioning of incident waves, and 2) A novel Fourier transform approach which, in a time-parallel manner and without causing spurious periodicity effects, delivers numerically dispersionless spectrally accurate solutions. A similar hybrid technique can be obtained on the basis of Laplace transforms instead of Fourier transforms, but we do not consider the Laplace-based method in the present contribution. The algorithm can handle dispersive materials, it can tackle complex physical structures and interface conditions (provided a correspondingly capable frequency-domain solver is used), it enables parallelization in time in a straightforward manner, and it allows for time leaping, that is, solution sampling at any given time T at $\mathcal{O}(1)$ -bounded sampling cost, for arbitrarily large values of T , and without requirement of evaluation of the solution at intermediate times. The proposed frequency/time hybridization strategy, which generalizes to any linear partial differential equation in the time domain for which frequency-domain solutions can be obtained (including e.g. the time-domain Maxwell equations), and which is applicable in a wide range of scientific and engineering contexts, provides significant advantages over volumetric discretization and convolution-quadrature approaches.

*e-mail: {tanderson,obruno}@caltech.edu, mark.lyon@unh.edu

1 Introduction

This paper proposes a fast frequency/time hybrid integral-equation method for the solution of the time domain wave equation in two- and three-dimensional spatial domains. Relying on 1) a smooth time-windowing methodology (for smooth time partitioning of incident waves), and 2) a novel FFT-accelerated Fourier transform approach (which, without requiring finer and finer meshes as time grows, is amenable to time parallelism and does not give rise to spurious periodicity effects), the proposed approach delivers numerically dispersionless solutions with numerical errors that decay faster than any power of the frequency mesh-size used. In practice the proposed methodology enjoys a number of attractive properties, including high accuracy without numerical dispersion error; an ability to effectively leverage existing frequency-domain scattering solvers for arbitrary spatial domains; dimensional reduction (if integral equation methods are used as the frequency domain solver components); natural parallel decoupling of the associated frequency-domain components; and, most notably, time-leaping, time parallelism, and $\mathcal{O}(1)$ cost for solution sampling at arbitrarily large times without requirement of intermediate time evaluation.

A wide literature exists, of course, for the treatment of the classical wave equation problem. Among the many approaches utilized in this context we find finite-difference and finite-element time domain methods [1, 2] (FDTD and FETD, respectively), retarded potential boundary integral equation methods [3–6], Huygens-preserving treatments for odd-dimensional spatial domains [7], and, most closely related to the present work, two hybrid frequency/time methodologies, namely, the Laplace-transform/finite-difference convolution quadrature method [8–13], and the Fourier-transform/operator-expansion method [14, 15]. A brief discussion of the character of these methodologies is presented in what follows.

The FDTD approach and related finite-difference methods underlie most of the wave-equation solvers used in practice: in these approaches the solution on the entire spatial domain is obtained via finite difference approximations of the PDE in both space and time. For the ubiquitous exterior-domain problems, the use of absorbing boundary conditions is necessary to render the problem computationally feasible—which has in fact been an important and challenging problem in itself [16–19]. Most importantly, however, finite-difference methods suffer from numerical dispersion, and they therefore require the use of fine spatial meshes (and, thus, fine temporal meshes, for stability) to produce accurate solutions. Numerical dispersion errors therefore present a significant obstacle for high frequency and/or long time simulations via methods based on finite-difference spatial discretizations. FETD methods provide an additional element of geometric generality, but they require creation of high-quality finite element meshes (which can be challenging for complex three-dimensional structures). Further, like FDTD methods, they entail use of absorbing boundary conditions, and they also generally give rise to detrimental dispersion errors (also called “pollution errors” in this context [20]).

Integral-equation formulations based on direct discretization of the time-domain retarded-potential Green’s function require treatment of the Dirac delta function and thus give rise to integration domains given by the intersection of the light cone with the overall scattering surface [3, 4, 7]. Huygens-preserving treatments of the retarded potential operators have the advantage that they do not entail an increasing amount of computational work for increasing time, at least in odd dimensions [7]. These approaches generally result in relatively complex overall schemes for which it has proven rather challenging to ensure stability [6], and which have typically been implemented in low-order accuracy setups and, thus, with significant numerical dispersion error [7]. Accelerated versions of these methods have also been proposed [5].

Hybrid time/frequency approaches rely on transform techniques to evaluate time domain solutions by synthesis from sets of frequency domain solutions. One of the most significant advantages

of these methods is that they allow for parallel solution of a set of frequency domain problems which are then recombined through a Laplace or Fourier transform, as appropriate, to produce the desired time domain solution. The Convolution Quadrature (CQ) method [8] is a prominent example of this class of approaches. The CQ method relies on the combination of a finite-difference time discretization and a Laplace transformation to effectively reduce the time domain wave equation to a set of modified Helmholtz equations over a range of frequencies. The overall cost and memory requirements of the CQ method grows linearly with the the number N of timesteps used to evolve the solution to a given final time T , and, therefore, the method requires large memory allocations for long time simulations. The approach has thus far been primarily used in conjunction with the second-order accurate BDF2 time discretization [9], but recent work [12] proposed the use of higher-order Runge-Kutta schemes which, for a scheme of stage order m utilize at least $\mathcal{O}(mN)$ frequency-domain solutions, with higher accuracies resulting from use of possibly significantly higher numbers of frequency domain solutions [13]. A key point is that the resulting time domain solution is itself *an approximation of the finite-difference approximation of the solution*. As a result, the solutions produced by this method inherit errors from each approximation step (along with, of course, the inevitable spatial discretization error). As discussed in Section 2.2.1, the approximation level inherent in the time-domain finite-difference discretization is only recovered by incorporating significant numbers of additional expensive frequency-domain solutions.

There has additionally been some interest in the direct use of Fourier transformations in time [14, 15] to decouple the time domain problem into frequency domain sub-problems. In detail, assuming a Gaussian-modulated incident time-pulse the approach [14, 15] evaluates the time evolution on the basis of a Gauss-Hermite quadrature rule. The resulting frequency-domain problems are solved by means of a certain “operator expansion method”. A significant difficulty arises in this method for the computation at advanced time, namely, that the Fourier integrand becomes increasingly oscillatory, requiring finer frequency discretizations and, therefore, larger numbers of associated frequency-domain solutions, as time grows—thus making long-time computation prohibitively expensive. Additional characteristics of and challenges inherent in hybrid frequency/time methods are discussed in some detail in Section 2.2.

In contrast, the proposed method uses a *time-windowed Fourier transformation* technique, which, we show, can always be re-centered in time to avoid high frequencies in the Fourier-transform domain ω . Many time-related properties of the proposed hybrid method emanate from the windowing approach, including time-parallel character, time-leaping and $\mathcal{O}(1)$ long time evaluation cost, $\mathcal{O}(N)$ cost for a total full N timestep history of the solution (while still remaining accurate in time for arbitrarily long times and with complete absence of dispersion error in time), and spectral time accuracy even for long incident pulses.

The proposed hybrid method relies on use of a sequence of smooth windowing functions (the sum of all of which equals unity) to smoothly partition time into a sequence of windowed time-intervals. Each new time evaluation requires summation of a fixed number of Fourier integrals which are computed efficiently, via consideration of a scaled convolution, on the basis of the Fractional Fourier Transform and the FFT. A similar hybrid technique can be obtained on the basis of Laplace transforms instead of Fourier transforms. Use of the Laplace-based technique would be advantageous for treatment of certain types of initial/boundary-value problems with non-vanishing initial conditions, but we do not consider this Laplace-based approach in any detail in the present contribution.

In order to achieve uniform accuracy in time, a new FFT-speed quadrature method for the evaluation of continuous Fourier transform integrals is presented, which does not require use of finer and finer discretization for accurate computation at larger and larger times (despite the increasingly oscillatory character of the integrands, as time passes, owing to the presence of the

Fourier exponential). Overall $\mathcal{O}(N)$ operations for N timesteps, on the other hand, results from use of relatively large, but bounded time window sizes W , so that each windowed incident field can be accurately discretized by means of a fixed number N_W of time-domain points.

The hybrid methodology described in the present contribution naturally lends itself to a number of trivial acceleration techniques via high-performance computing. First, the method naturally reduces the solution into multiple frequency-domain problems which are entirely decoupled and thus naturally solved in parallel. Next, the production of near-field time-domain solution are spatially-decoupled, with the solution at each point depending only on boundary densities. The time parallelism, finally, can also be exploited through the smooth time-partitioning approach, so that only the relevant parts of a wave's phenomena are computed. All three of these decoupling techniques lead directly to embarrassingly-parallel algorithms. Finally, parallel versions of existing high-performance solvers [21, 22] for the frequency-domain integral equation problems are readily usable.

This paper is organized as follows. After certain necessary preliminaries are presented in Section 2, the three main components of the proposed approach are taken up in Sections 3 through 5. Thus Section 3 reviews well known frequency and time domain integral formulations of the wave-equation problem, Section 4 introduces the smooth time-windowing technique that underlies the proposed accelerated treatment of signals of arbitrary long duration, and Section 5 puts forth a new quadrature rule for the spectral evaluation of Fourier transform integrals at FFT speeds, with high-order accuracy and $\mathcal{O}(1)$ large-time sampling costs. A variety of numerical results, finally, are presented in Section 6. We believe that, in view of its spectral time accuracy, absence of stability constraints, fast algorithmic implementations, easy use in conjunction with any existing frequency-domain solver, and bounded memory requirements, the proposed method should prove attractive in a number of contexts in science and engineering. The ideas developed may be applied to any time-domain problem whose frequency-domain counterpart can be treated by means of either a spatial fast Green's function method or some other efficient frequency-domain approach.

2 Preliminaries

2.1 Differential and integral wave-equation formulations

We consider the initial boundary value problem

$$\frac{\partial^2 u}{\partial t^2}(\mathbf{r}, t) - c^2 \Delta u(\mathbf{r}, t) = 0, \quad \mathbf{r} \in \Omega, \quad (1a)$$

$$u(\mathbf{r}, 0) = \frac{\partial u}{\partial t}(\mathbf{r}, 0) = 0 \quad (1b)$$

$$u(\mathbf{r}, t) = h(\mathbf{r}, t) \quad \text{for } (\mathbf{r}, t) \in \Gamma \times [0, T^{inc}], \quad (1c)$$

for the time domain wave equation in the domain $\Omega \subset \mathbb{R}^d$ ($d = 2, 3$) with boundary Γ . For definiteness, throughout this paper we assume the boundary condition (1c). Given a spatial incident field

$$u^{tot}(\mathbf{r}, t) = u^{inc}(\mathbf{r}, t) + u(\mathbf{r}, t) = 0, \quad \mathbf{r} \in \Gamma$$

the selection $h = -u^{inc}$ corresponds to a sound soft boundary condition for the total field $u + u^{inc}$ on the boundary of the scatterer. Of course, other boundary conditions can be also be considered in our context without difficulty.

Although not explicitly used as part of the proposed algorithm, it is useful here to recall the single-layer integral representation formula

$$u(\mathbf{r}, t) = \int_{-\infty}^t \int_{\Gamma} G(\mathbf{r} - \mathbf{r}', t - t') \varphi(\mathbf{r}', t') d\sigma(\mathbf{r}') dt', \quad (2)$$

which yields the solution u throughout Ω in terms of the time-dependent boundary density φ and the time-domain Green's function

$$G(\mathbf{r}, t) = \begin{cases} \frac{H(ct - |\mathbf{r}|)}{2\pi\sqrt{(ct)^2 - |\mathbf{r}|^2}} & \text{for } d = 2 \text{ and} \\ \frac{\delta(ct - |\mathbf{r}|)}{4\pi|\mathbf{r}|} & \text{for } d = 3. \end{cases} \quad (3)$$

for equation (1). Here $\delta(t)$ and $H(t)$ denote the classical delta and Heaviside functions ($H(t)$ equals zero or one depending on whether $t < 0$ or $t > 0$, respectively), and $d\sigma(\mathbf{r}')$ denotes the area element on the $(d - 1)$ -dimensional surface Γ . As is known, the single layer potential (2) is a solution of the initial and boundary value problem (1) if and only if φ satisfies the time domain boundary integral equation

$$\int_{-\infty}^t \int_{\Gamma} G(\mathbf{r} - \mathbf{r}', t - t') \varphi(\mathbf{r}', t') d\sigma(\mathbf{r}') dt' = h(\mathbf{r}, t) \quad \text{for } (\mathbf{r}, t) \in \Gamma \times [0, T^{inc}]. \quad (4)$$

2.2 Previous hybrid methods: Convolution quadrature [8] and direct Fourier transform in time [14]

As mentioned in Section 1, two hybrid time-domain methods (i.e., methods that rely on transformation of the time variable by means of Fourier or Laplace transforms) have previously been proposed. The Convolution Quadrature method [8–13] uses a discrete convolution that results as a temporal finite-difference schemes are solved by transform methods. Like the method introduced in the present contribution, in turn, the direct Fourier transform method [14, 15] is based on direct Fourier synthesis of time-harmonic solutions.

2.2.1 Convolution quadrature

In detail, the Convolution Quadrature method considers the forward recurrence relation arising from finite difference time-stepping methods and proceeds by application of the Z-transform on the discrete time variable. Utilizing the Z-transform frequency domain, a finite-difference time discretization of the wave equation can be reformulated as a set of modified Helmholtz problems. The discrete time domain solution is then given by evaluating a trapezoidal-rule quadrature for the inverse Z-transform of these frequency domain solutions. References [8] and [13] provide further elaboration on the connections to convolutions and Z-transforms, respectively. A key point is that the resulting time domain solution is *an approximation of the time-domain finite-difference approximation of the solution*. As a result, the solutions produced by this method inherit errors from each approximation step (along with, of course, the inevitable spatial discretization error). As shown in [13], the errors in the first approximation (via trapezoidal rule quadrature of a contour integral) can be mitigated (at the cost of significant numbers of expensive frequency-domain solutions, with frequency numbers that grow as the time-step is refined) so that the original time-domain finite-difference approximation error is recovered. A brief discussion of the nature of these approximation errors follows.

In the context of wave propagation, it is not only asymptotic convergence order which affects the behavior of numerical schemes: the numerical dispersion error introduced by time-domain finite

difference discretizations plays a fundamental role—as described in [11, 23] for the convolution-quadrature approach. In fact to avoid significant dissipation error arising from linear multistep schemes such as BDF2, the timestep must be chosen to vary quadratically with frequency [11]. While higher-order methods, especially the Runge-Kutta class, may be used to manage these errors, published numerical results still show significant dispersion error even for time histories of moderate length [10]. An important motivation of our efforts is the development of an approach that eliminates dispersion errors.

A significant and well-known drawback of the Convolution-Quadrature approach concerns its infinite time-tail- [7]. For example, in [24, Chapter 5] we read:

The sequence of problems [...] presents the serious disadvantage of having an infinite tail. In other words, the passage through the Laplace domain introduces a regularization of the wave equation that eliminates the Huygens principle that so clearly appears in the time domain retarded operators and potentials.

This increasing tail corresponds to an increasing amount of computational work in numerical solvers. Reference [7] makes note of this fact, and indeed relies on the strong Huygens principle in three spatial dimensions to derive a formulation recovering the attractive shorter-range dependence properties.

2.2.2 Direct Fourier transform in time

Without reliance on finite difference approximations, direct Fourier transform methods proceed by Fourier transformation of the time domain wave equation followed by solution of the resulting Helmholtz equations for a range of frequencies, and are completed by inverse transformation to the time-domain. Importantly, a direct Fourier method does not suffer from dispersion errors in the time variable (provided, of course, that suitable quadrature rule are used). Use of the direct approach is proposed in Mecocci et al. [14]. In that contribution the needed Helmholtz solutions are obtained by means of a certain “operator-expansion” technique, and, assuming the incident field is given by a plane wave modulated by a Gaussian envelope in frequency domain, the needed Fourier integrals are approximated using the classical Gauss-Hermite quadrature rule.

Except for simple geometries, the use of the operator-expansion method limits the overall accuracy to the point that in many cases it is difficult to discern convergence. This difficulty could be of course resolved by switching to a more effective modern frequency-domain technique. Most significantly, however, use of any generic numerical integration procedure, including the highly accurate Gauss-Hermite rule, does lead to difficulties: 1) As time grows the integrands in the needed Fourier-transform integrals becomes more and more oscillatory, thus requiring use of finer and finer discretizations (each one of whose discretization points requires an expensive solution of a frequency-domain problem), and 2) The overall integration cost grows quadratically with the size of the time-interval considered (or, more precisely, grows quadratically with the inverse of the smallest time-step used)—as opposed to the linear-time required by other numerical methods. Therefore, the direct Fourier transform method does not generally provide an effective time-domain solver.

In presence of the Gaussian-windowed integrands considered in Mecocci et al. [14] use of trapezoidal rule integration might appear advantageous—since, for such integrands, the trapezoidal rule exhibits superalgebraically fast convergence and crucially it can be evaluated by means of FFTs. Unfortunately, as is well known, this is not a viable approach: unfortunately, like the aforementioned Gauss-Hermite rule, the trapezoidal rule also requires use of finer and finer meshes as frequencies increase: failure to increase the frequency-sampling rate would give rise to $\mathcal{O}(1)$ aliasing errors. In

detail, using the convention

$$F(\omega) = \int_{-\infty}^{\infty} f(t)e^{i\omega t} dt, \quad f(t) = \frac{1}{2\pi} \int_{-\infty}^{\infty} F(\omega)e^{-i\omega t} d\omega \quad (5)$$

for the Fourier transform pair, and assuming an e.g. $T/2$ -time-limited function f , with an equi-spaced sampling in both time and frequency space of $t_j = (j - m/2), \omega_k = 2\pi(k - m/2)/T, 0 \leq j, k < m$, the trapezoidal rule yields

$$F(\omega_k) = \int_{-\infty}^{\infty} f(t)e^{it\omega_k} dt = \int_{-T/2}^{T/2} f(t)e^{it\omega_k} dt \approx \frac{T}{m} \sum_{j=0}^{m-1} f(t_j)e^{it_j\omega_k} \quad (6)$$

$$= \frac{T}{m} e^{-\pi i(k-m/2)} \sum_{j=0}^{m-1} f(t_j)e^{-\pi i j} e^{2\pi i j k/m}. \quad (7)$$

The trapezoidal rule is attractive because as presented in (7) it enables use of the FFT (other methods to handle the oscillatory integrand such as Filon’s integration rule have not been accelerated to FFT speeds, and as well possess only fixed-order convergence). Equation (6) clearly displays $F(\omega_k)$ as a periodic function of k (while the actual Fourier transform may have an arbitrarily prescribed frequency dependence)—which is a manifestation of aliasing errors in the present context. Zero-padding resolves the difficulty, at the expense, once again, of fine frequency meshes and large numbers of frequency-domain solutions.

The efficient method proposed in this paper resolves these fundamental difficulties: it eliminates aliasing errors (and it yields superalgebraically fast convergence as the relevant discretization is refined) without recourse to zero padding, and it evaluates the time-domain solution by means of FFTs—so that, as in finite-difference time discretizations, the overall cost of the time propagation algorithm is proportional to the number of steps used in time.

2.2.3 Computational complexity of hybrid methods

The total computing costs required by a given hybrid algorithm will be quantified in terms of the number N of degrees of freedom used to discretize time and an upper-bound M on the number of operations required by each one of the necessary frequency-domain solutions—which comprise the bulk of the cost of all hybrid methods.

The Convolution-Quadrature method with either a BDF2 or a Runge-Kutta time discretization requires (up to logarithmic terms) $\mathcal{O}(N \log(N)M)$ operations [9, Sec. 4]. Similarly, the direct frequency superposition method requires $\mathcal{O}(NM) + \mathcal{O}(N^2)$ operations (owing to the increasingly oscillatory nature of frequency domain problems as time grows, for the first term, and on account of the Gauss-Hermite integration for Fourier transformation at each temporal discretization point, for the second term). In contrast, as shown in Section 5, the proposed fast hybrid method requires $rM + \mathcal{O}(N)$ operations to evaluate the solution at N time points (where r is the number, independent of N , of frequency-domain solutions required by the method to reach a given accuracy for arbitrarily long time).

Note that while the previous hybrid methods require the solution of an increasing number of Helmholtz problems as time grows, the proposed method does not—a fact which lies at the heart of the claimed $\mathcal{O}(1)$ -in-time sampling cost for arbitrarily large times t . In terms of memory storage, the fast hybrid method requires rV memory units for sampling at arbitrarily large times, where V denotes an upper bound for the storage needed for each one of the necessary frequency-domain solutions. Of course, storage of the entire time history on a given set of spatial points does require an additional $\mathcal{O}(N)$ memory units.

3 Frequency-domain representation

As is well-known, Fourier transformation in time of the time domain wave equation with frequency variable ω results in the Helmholtz equation (for whose numerical solution a wide literature has been developed),

$$\begin{aligned}\Delta U(\mathbf{r}) + \frac{\omega^2}{c^2}U(\mathbf{r}) &= 0, \quad \mathbf{r} \in \Omega \\ U(\mathbf{r}) &= H(\mathbf{r}), \quad \mathbf{r} \in \Gamma.\end{aligned}\tag{8}$$

A common approach of solution is via the method of layer potentials; to this end, we define the frequency-domain single and adjoint double-layer operators

$$(S_\omega\psi)(\mathbf{r}) = \int_\Gamma G_{\omega/c}(\mathbf{r}, \mathbf{r}')\psi(\mathbf{r}')d\sigma(\mathbf{r}'), \quad \mathbf{r} \in \Gamma, \tag{9}$$

$$(K_\omega^*\psi)(\mathbf{r}) = \int_\Gamma \frac{\partial G_{\omega/c}(\mathbf{r}, \mathbf{r}')}{\partial n(\mathbf{r})}\psi(\mathbf{r}')d\sigma(\mathbf{r}'), \quad \mathbf{r} \in \Gamma, \tag{10}$$

where G_ω denotes the fundamental solution of the Helmholtz equation at frequency ω —which in the two- and three-dimensional cases is given, respectively, by

$$G_\omega(r, r') = \frac{i}{4}H_0^{(1)}\left(\frac{\omega}{c}|r - r'|\right) \quad \text{and} \quad G_\omega(r, r') = \frac{e^{i\frac{\omega}{c}|r - r'|}}{4\pi|r - r'|}.\tag{11}$$

As mentioned above, a frequency domain formulation for the problem (1) follows from Fourier transformation of the time variable,

$$u(\mathbf{r}, t) = \frac{1}{2\pi} \int_{-\infty}^{\infty} U(\mathbf{r}, \omega)e^{-i\omega t}d\omega, \quad \mathbf{r} \in \Omega, \tag{12}$$

and use of the “physical” frequency domain field representation

$$U(\mathbf{r}, \omega) = \int_\Gamma \psi(\mathbf{r}', \omega)G_\omega(\mathbf{r}, \mathbf{r}')d\sigma(\mathbf{r}'), \quad \mathbf{r} \in \Omega, \tag{13}$$

where, for each ω , the boundary integral density $\psi(\mathbf{r}, \omega) = \frac{\partial U(\mathbf{r}, \omega)}{\partial n(\mathbf{r})}$ is the solution of the direct integral equation

$$(S_\omega\psi)(\mathbf{r}, \omega) = H(\mathbf{r}, \omega), \quad \mathbf{r} \in \Gamma. \tag{14}$$

Unfortunately, equation (14) is not uniquely solvable for certain values of ω . Making use of the auxiliary double-layer integral equation for the same physical density ψ (which is also non-invertible at certain frequencies),

$$\frac{1}{2}\psi(\mathbf{r}, \omega) - (K_\omega^*\psi)(\mathbf{r}, \omega) = -\frac{\partial H(\mathbf{r}, \omega)}{\partial n(\mathbf{r})}, \quad \mathbf{r} \in \Gamma, \tag{15}$$

we obtain the *uniquely solvable* direct combined field integral equation formulation (see e.g. [25]):

$$\frac{1}{2}\psi(\mathbf{r}, \omega) - (K_\omega^*\psi)(\mathbf{r}, \omega) - i\eta(S_\omega\psi)(\mathbf{r}, \omega) = -\left(\frac{\partial H(\mathbf{r}, \omega)}{\partial n(\mathbf{r})} + i\eta H(\mathbf{r}, \omega)\right), \quad \mathbf{r} \in \Gamma. \tag{16}$$

The boundary integral equation presented here can be tackled numerically with a variety of approaches and acceleration strategies. In this paper we use the well-known Nyström quadrature

method to discretize and solve the integral equations (16) for all desired frequencies; details can be found in, e.g., [26].

As is well known, the time-domain Green's function and associated integral formulation (equations (2) through (4)) are closely related to the corresponding frequency-domain representation (12) and equation (14) in both the two- and three-dimensional cases ($d = 2$ and $d = 3$). The derivation is fairly straightforward. We consider the somewhat simpler $d = 3$ case first. Substituting (13) into (12) yields

$$\begin{aligned} u(\mathbf{r}, t) &= \frac{1}{2\pi} \int_{-\infty}^{\infty} e^{-i\omega t} \int_{\Gamma} \psi(\mathbf{r}', \omega) G_{\omega}(\mathbf{r}, \mathbf{r}') d\sigma(\mathbf{r}') d\omega, \\ &= \frac{1}{2\pi} \int_{\Gamma} \int_{-\infty}^{\infty} \psi(\mathbf{r}', \omega) \frac{e^{i\omega/c|\mathbf{r}-\mathbf{r}'|}}{|\mathbf{r}-\mathbf{r}'|} e^{-i\omega t} d\omega d\sigma(\mathbf{r}'), \quad \mathbf{r} \in \Omega. \end{aligned}$$

Then owing to the Fourier transform relation

$$\frac{1}{4\pi} \frac{e^{i\frac{\omega}{c}|\mathbf{r}-\mathbf{r}'|}}{|\mathbf{r}-\mathbf{r}'|} e^{-i\omega t} = \int_{-\infty}^t \frac{\delta(c(t-t') - |\mathbf{r}-\mathbf{r}'|)}{4\pi|\mathbf{r}-\mathbf{r}'|} e^{-i\omega t'} dt',$$

together with the relation that the Fourier transform of $\psi = \frac{\partial U}{\partial n}$, is the time-dependent normal derivative of the scattered field on the boundary φ ,

$$\varphi(\mathbf{r}, t) = \frac{\partial u(\mathbf{r}, t)}{\partial n(\mathbf{r})} = \frac{1}{2\pi} \int_{-\infty}^{\infty} \psi(\mathbf{r}, t) e^{-i\omega t} d\omega \quad (17)$$

we have,

$$u(\mathbf{r}, t) = \int_{-\infty}^t \int_{\Gamma} G(\mathbf{r}-\mathbf{r}', t-t') \varphi(\mathbf{r}', t') d\sigma(\mathbf{r}') dt', \quad \mathbf{r} \in \Omega, \quad (18)$$

which coincides with the time domain single layer representation formula (2), the classical Kirchhoff formula [27, Chap. VIII].

In the case of $d = 2$, in turn, we have

$$u(\mathbf{r}, t) = \frac{1}{2\pi} \int_{\Gamma} \int_{-\infty}^{\infty} \psi(\mathbf{r}', \omega) e^{-i\omega t} \frac{i}{4} H_0^{(1)}\left(\frac{\omega}{c}|\mathbf{r}-\mathbf{r}'|\right) d\omega \quad (19)$$

Introducing the integral representation

$$H_{\nu}^{(1,2)}(z) = \pm \frac{2e^{\mp\nu\pi i}}{i\sqrt{\pi}\Gamma(\nu + \frac{1}{2})} \left(\frac{z}{2}\right)^{\nu} \int_1^{\infty} e^{izt} (t^2 - 1)^{\nu-1/2} dt, \quad \Re(\nu) > -\frac{1}{2}$$

for the Hankel functions of the first and second kind [28, form. 5.10.20-21], it follows that the first-kind Hankel function appearing in equation (19) may be expressed, after appropriate changes of variables, in the form

$$H_0^{(1)}\left(\frac{\omega}{c}|\mathbf{r}-\mathbf{r}'|\right) = -\frac{2i}{\pi} \int_{|\mathbf{r}-\mathbf{r}'|}^{\infty} \frac{e^{i\tau\omega/c}}{\sqrt{\tau^2 - |\mathbf{r}-\mathbf{r}'|^2}} d\tau.$$

Substituting this relation into (19) yields

$$u(\mathbf{r}, t) = \frac{1}{2\pi} \int_{\Gamma} \int_{-\infty}^{\infty} \psi(\mathbf{r}, t) e^{-i\omega t} \int_{|\mathbf{r}-\mathbf{r}'|}^{\infty} \frac{e^{i\omega\tau/c}}{2\pi\sqrt{\tau^2 - |\mathbf{r}-\mathbf{r}'|^2}} d\tau d\omega d\sigma(\mathbf{r}') \quad (20)$$

$$= \frac{1}{2\pi} \int_{-\infty}^{\infty} \int_{-\infty}^t \int_{\Gamma} \frac{H(c(t-t') - |\mathbf{r} - \mathbf{r}'|) \psi(\mathbf{r}', \omega) e^{-i\omega t'}}{2\pi \sqrt{c^2(t-t')^2 - |\mathbf{r} - \mathbf{r}'|^2}} d\sigma(\mathbf{r}') dt' d\omega, \quad (21)$$

which, in view of (3), yields the desired $d = 2$ single layer representation formula (2), the Kirchhoff formula [29, §6]:

$$u(\mathbf{r}, t) = \int_{-\infty}^t \int_{\Gamma} G(\mathbf{r} - \mathbf{r}', t - t') \varphi(\mathbf{r}', t') d\sigma(\mathbf{r}') dt', \quad \mathbf{r} \in \Omega. \quad (22)$$

Remark 1. In Section 4 we exploit the physical character of the density to determine the times at which contributions from various incident-field time windows can be neglected (without violating a prescribed error tolerance) for a given observation point or, more generally, for given regions in space.

4 Smooth time-partitioning strategy

4.1 Time partitioning and the Fourier Transform: general elements

Considering the Fourier transform pair (5), let $F(\omega)$ be the Fourier Transform of some (finitely or infinitely) smooth compactly supported function $u(t)$, assumed zero except for $t \in [0, T]$ ($T > 0$) (as there arise, e.g., in the smooth time-partitioning strategy described in Section 4.2). In this case the Fourier transform is given by an integral over a finite (but potentially large) time interval:

$$F(\omega) = \int_0^T f(t) e^{i\omega t} dt. \quad (23)$$

The inverse Fourier transform, in turn, is

$$f(t) = \frac{1}{2\pi} \int_{-\infty}^{\infty} F(\omega) e^{-i\omega t} d\omega. \quad (24)$$

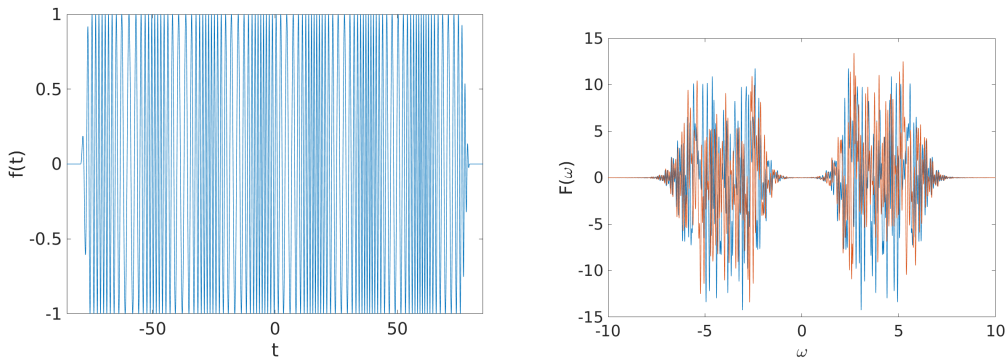


Figure 1: Long duration time signal $f(t)$ on the left with its corresponding and highly oscillatory Fourier Transform $F(\omega)$ on the right. It may be useful to note the windowing in the time signal depicted on the left. The right-blue and right-red plots depict the real and imaginary parts of the Fourier Transform, respectively.

In the context of our problem it is useful to consider the variation in the oscillatory character of $F(\omega)$ on the length T of the interval within which f is allowed to differ from zero. Indeed, as

demonstrated by Figure 1, for large values of T , the function $F(\omega)$ (right image) is generically highly oscillatory—owing to the presence of the factor $e^{i\omega t}$, for t large, in the integrand displayed in equation (23): loosely speaking, $F(\omega)$ is a “linear combination” of exponential functions of ω which are highly oscillatory for large t . The consequence is that a very fine discretization mesh ω_j , containing $\mathcal{O}(T)$ elements, would be required to obtain $f(t)$ from $F(\omega)$ on the basis of (24). In the context of a hybrid frequency-time solver, this would entail use of a number $\mathcal{O}(T)$ of applications of the most expensive part of the overall algorithm: the boundary integral equations solver—which would make the overall time-domain algorithm unacceptably slow. This section describes a new Fourier transform algorithm that produces $f(t)$ (left image in Figure 1) within a prescribed accuracy tolerance, and for any value of T , however large, by means of a T -independent (small) set of discrete frequency values ω_j ($-W \leq \omega_j \leq W$, $j = 0, \dots, J$).

In order to introduce the proposed strategy for the large- T Fourier transform problem, let s_k ($1 \leq k \leq K$) denote a set of equi-spaced values (the “centers of the windowing functions”) in the interval $[0, T]$, let $H > 0$ be a “small” (or, more precisely, a T -independent) real number, and let $\mathcal{P} = \{w_k(t) | k = 1, \dots, K\}$ denote a set of non-negative smooth windowing functions $w_k(t)$ which satisfy

- a) $w_k(t) = 1$ in a neighborhood of $t = s_k$,
- b) $w_k(t) = 0$ for $|t - s_k| > H$, and
- c) $\sum_{k=1}^K w_k(t) = 1$ for all $t \in [0, T]$.

In view of point c) we call \mathcal{P} a smooth partition of unity over the interval $[0, T]$. Note that the integer K is an $\mathcal{O}(T)$ quantity and, in particular, it is not independent of T .

Using the partition of unity \mathcal{P} , for $\omega \in [-W, W]$ we may write

$$F(\omega) = \sum_{k=1}^K F_k(\omega), \quad \text{where} \quad F_k(\omega) = \int_0^T w_k(t) f(t) e^{i\omega t} dt. \quad (25)$$

But, letting

$$f_k(t) = w_k(t) f(t), \quad (26)$$

we clearly have

$$F_k(\omega) = \int_{s_k-H}^{s_k+H} f_k(t) e^{i\omega t} dt = e^{i\omega s_k} F_k^{slow}(\omega) \quad (27)$$

where

$$F_k^{slow}(\omega) = \int_{-H}^H f_k(t + s_k) e^{i\omega t} dt = \int_{-H}^{\infty} f_k(t + s_k) e^{i\omega t} dt = e^{-i\omega s_k} \int_{-\infty}^{\infty} f_k(v) e^{i\omega v} dv. \quad (28)$$

The “slow” superscript refers to the fact that, since t in (28) is “small” (it satisfies $-H \leq t \leq H$), it follows that the integrand (28) only contains slowly oscillating exponential functions of ω , and thus $F_k^{slow}(\omega)$ is itself slowly oscillatory. Thus (27) expresses $F_k(\omega)$ as product of two terms: the highly oscillatory exponential term $e^{i\omega s_k}$ (which arises from the fact that the support of the signal is not centered around the origin *in time*, but not from any actual high-frequency character in the signal f), on one hand, and the slowly oscillatory term $F_k^{slow}(\omega)$.

In view of the smoothly-windowed integrand in (28), integration by parts yields

$$|F_k^{slow}(\omega)| \leq \omega^{-p} \int_{-H}^H |f_k^{(p)}(t + s_k)| dt \leq \omega^{-p} \|f_k^{(p)}\|_{L^1[-\infty, \infty]} \leq C \omega^{-p} \|f^{(p)}\|_{L^1[-\infty, \infty]}, \quad (29)$$

where the constant $C = C(H, p)$ is independent of k . In other words, $F_k^{slow}(\omega)$ decays superalgebraically fast as $\omega \rightarrow \pm\infty$ uniformly in k .

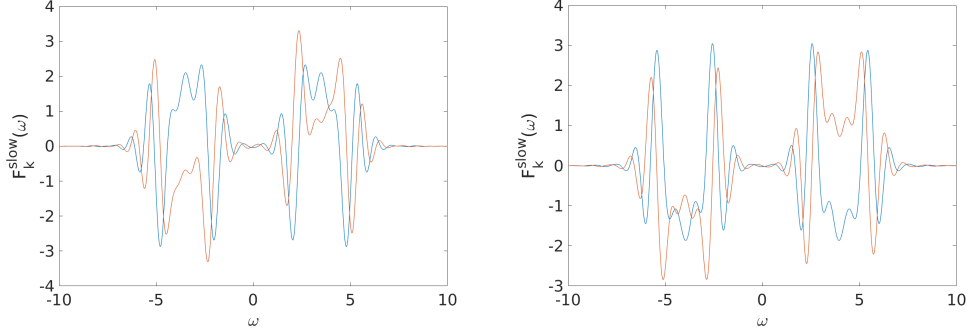


Figure 2: Fourier Transform of two windowed regions of the long duration signal shown in Figure 1, each with window width $H = 10$. The left and right figures depict the transform corresponding, respectively, to a window center of $s_k = 0$ and $s_k = -55$. In each case, the blue and red plots depict the real and imaginary parts of the Fourier Transform, respectively.

4.2 Efficient time-partitioning algorithmic strategy

In order to evaluate numerically the solution of the problem (1), we apply the Fourier transform formalism developed in Section 4.1 to the function $h(\mathbf{r}, t)$, in the t variable, for each fixed value of \mathbf{r} . For each k equation (27) and (28) become

$$H_k(\mathbf{r}, \omega) = \int_{-\infty}^{\infty} w_k(t) h(\mathbf{r}, t) e^{i\omega t} dt, \quad (30)$$

and

$$H_k^{slow}(\mathbf{r}, \omega) = e^{-i\omega s_k} H_k(\mathbf{r}, \omega). \quad (31)$$

It is easy to check that the solutions $u(\mathbf{r}, t)$ and $u_k(\mathbf{r}, t)$ to the problem (1) with $h(\mathbf{r}, t) = f(\mathbf{r}, t)$ and $h(\mathbf{r}, t) = w_k(t)f(\mathbf{r}, t)$, respectively, satisfy

$$u(\mathbf{r}, t) = \sum_{k=1}^K u_k(\mathbf{r}, t). \quad (32)$$

Applying (12) to $u_k(\mathbf{r}, t)$ for $1 \leq k \leq K$ and using (31) we obtain

$$u_k(\mathbf{r}, t) = \frac{1}{2\pi} \int_{-\infty}^{\infty} U_k(\mathbf{r}, \omega) e^{-i\omega t} d\omega = \frac{1}{2\pi} \int_{-\infty}^{\infty} U_k^{slow}(\mathbf{r}, \omega) e^{-i\omega(t+s_k)} d\omega,$$

where the functions $U_k(\mathbf{r}, \omega)$ and $U_k^{slow}(\mathbf{r}, \omega)$ are solutions of Helmholtz problem (8) with $H = H_k$ and $H = H_k^{slow}$, respectively.

In order to obtain an integral over a bounded domain (and, thus, to enable discretization of the integral by means of a finite number of frequency-domain samples) we introduce the truncated version

$$u_k^W(\mathbf{r}, t) = \frac{1}{2\pi} \int_{-W}^W U_k^{slow}(\mathbf{r}, \omega) e^{-i\omega(t+s_k)} d\omega \quad (33)$$

of u_k . Applying (29) to $f = h$ tells us that, for each fixed \mathbf{r} , the function $H_k^{slow}(\mathbf{r}, \omega)$ is superalgebraically small as $\omega \rightarrow \infty$. A consequence is that the approximation (33) possesses errors that decay faster than any power of W , as $W \rightarrow \infty$, uniformly for all k and for all real values of t . Thus, relying on the values $U_k^{slow}(\omega_j)$ on a k -independent set $\{\omega_1, \dots, \omega_J\}$ containing J frequency-discretization

points, the quadrature rule presented in Section 5.1 provides an approximation $u_k^{W,J}(t)$ for the integral (33) with errors that are superalgebraically small, uniformly in time, provided W and J are sufficiently large. Summing over k for the K partitions in \mathcal{P} and using (32) we obtain the approximation

$$u(\mathbf{r}, t) = \sum_{k=1}^K u_k(\mathbf{r}, t) \approx \sum_{k=1}^K u_k^{W,J}(\mathbf{r}, t) \quad (34)$$

for all $t > 0$, with superalgebraically-small t -uniform errors for all $t > 0$ —a highly desirable characteristic of the proposed smooth time-partitioning strategy.

The expression (33) for the time-domain functions $u_k^W(\mathbf{r}, t)$ in terms of the frequency-domain solutions $U_k^{slow}(\mathbf{r}, \omega)$ can be exploited, in conjunction with (34), to design an efficient algorithm for the evaluation of the desired solution $u(\mathbf{r}, t)$ for given boundary values $h(\mathbf{r}, t)$. In the simplest implementation, for example, we may consider, for a prescribed frequency modulation function A , a W -band-limited function $h(\mathbf{r}, t)$ which is given by a linear combination

$$h(\mathbf{r}, t) = \frac{1}{2\pi} \int_{-\infty}^{\infty} H(\mathbf{r}, \omega) e^{-i\omega t} d\omega = \frac{1}{2\pi} \int_{-\infty}^{\infty} A(\omega) e^{i\omega(\mathbf{p}\cdot\mathbf{r}-t)} d\omega, \quad (35)$$

of plane waves, all of which share a single incidence direction \mathbf{p} . In this case, a single set of frequency domain solutions satisfying the boundary conditions $H_0(\mathbf{r}, \omega) = e^{i\omega\mathbf{p}\cdot\mathbf{r}}$ for a fixed set of frequencies $\{\omega_1, \dots, \omega_J\}$ can be used to produce u_k for all k (and, thus, $u(\mathbf{r}, t)$ for all t). This re-utilization of a “small” number of frequency-domain solutions is a key element leading to the efficiency of the proposed algorithm for incident signals of arbitrarily-long duration.

Of course, for a fully generic wave equation solver we must consider general boundary conditions $h(\mathbf{r}, t)$. In this case we may use a similar approach, on the basis of plane-wave representation [30, Chap. 1.2] and [21]

$$h(\mathbf{r}, t) = \frac{1}{(2\pi)^4} \int_{-\infty}^{\infty} \int_{\mathbb{R}^d} H(\mathbf{p}, \omega) e^{i(\mathbf{p}\cdot\mathbf{r}-\omega t)} d\mathbf{p} d\omega \quad (36)$$

$$H(\mathbf{p}, \omega) = \int_{-\infty}^{\infty} \int_{\mathbb{R}^d} h(\mathbf{r}, \omega) e^{-i(\mathbf{p}\cdot\mathbf{r}-\omega t)} d\mathbf{r} d\omega \quad (37)$$

4.3 Tracking of active time-windows

Significant additional efficiency can be gained in the frequently-encountered cases in which the k -th windowed solution u_k^W becomes negligible throughout the relevant spatial domain in finite time: once such vanishing is detected for the solution u_k^W , this k -th solution need no longer be computed numerically. The vanishing behavior of the solution u_k^W can be easily tracked via consideration of the expression (22) specialized to u_k^W and corresponding time windows of the form $[T_i + r_{min}/c, T_f + r_{max}/c]$ where r_{min} , r_{max} are, respectively, the minimum and maximum distance between a given evaluation point and the scattering configuration, and where T_i and T_f the initial and final time for which the k -th scattered field u_k^W does not vanish on the scattering boundary.

5 High-order $\mathcal{O}(1)$ large-time Fourier transform sampling at FFT speed

5.1 Smooth $F(\omega)$: FFT-based reduction to “scaled convolution”

Once solutions to (16) have been produced for an adequate range of frequencies ω , the time domain solution $u(\mathbf{r}, t)$ can be obtained, in view of (12) and, for long duration incident fields, the

time-windowing strategy described in Section 4, by inverse Fourier transformation. This section introduces an algorithm for the accurate quadrature, $\mathcal{O}(1)$ large-time sampling, and long-time computation at FFT-speeds of such Fourier transform integrals—a combined capability that, as discussed in Section 2, is not provided by previous algorithms—in the case that $F = F(\omega)$ is a smooth function of ω . The approach proceeds by resorting to certain “scaled convolutions”; a fast FFT-based algorithm for evaluation of such convolution-like quantities is described in Section 5.2. Section 5.3 then considers cases in which F is not smooth—as there arise for two-dimensional configurations under certain circumstances.

5.1.1 Symmetric integration intervals

In what follows we thus consider integrals which, like the right-hand side in (12), and in view of the time-windowing strategy described in Section 4, can be expressed in the form

$$f(t) = \int_{-\infty}^{\infty} F(\omega)e^{-i\omega t} d\omega = \int_{-W}^W F(\omega)e^{-i\omega t} d\omega \quad (38)$$

where f is a band-limited function with a smooth Fourier transform supported in the interval $[-W, W]$. (A non-smooth point that arises at $\omega = 0$ in the two-dimensional case is separately discussed in Section 5.3.)

Thus, substituting $F(\omega)$ by its truncated Fourier series approximation of period $2W$,

$$F(\omega) = \sum_{m=-N/2}^{N/2-1} c_m e^{i\frac{\pi}{W}m\omega}$$

(whose approximation errors tend to zero super-algebraically fast, i.e., faster than any negative power of N [31, Lemma 7.3.3]), and integrating term-wise yields the super-algebraically accurate approximation

$$\begin{aligned} f(t) &\approx \sum_{m=-N/2}^{N/2-1} c_m \int_{-W}^W e^{i\frac{\pi}{W}(m-\frac{W}{\pi}t)\omega} d\omega = \sum_{m=-N/2}^{N/2-1} c_m \left[\frac{2\alpha}{\alpha t - m} \sin\left(\frac{(\alpha t - m)W}{\alpha}\right) \right] \\ &= \sum_{m=-N/2}^{N/2-1} c_m (2W \operatorname{sinc}(\alpha t - m)), \end{aligned} \quad (39)$$

where we have set $\alpha = W/\pi$. Note that, paralleling the fast Fourier series convergence, the last expression in (39) provides a super-algebraically close approximation of $f(t)$ that, additionally, is uniform in t : for a given error tolerance ε there exists an integer N such that the approximation errors are less than ε for all real values of t . In view of (39), for a *given* equi-spaced time-evaluation grid $\{t_\ell = \ell\Delta t\}_{\ell=L_1}^{L_2}$ we may write

$$f(t_\ell) \approx \sum_{m=-N/2}^{N/2-1} c_m b_{\beta\ell-m}, \quad \text{where } \beta = \frac{W}{\pi}\Delta t \quad \text{and} \quad b_q = 2W \operatorname{sinc}(q). \quad (40)$$

The sum expression in (40) is a “scaled convolution” of c_m and b_q which, as indicated in Section 5.2, can be evaluated at FFT speeds [32].

5.1.2 Non-symmetric integration intervals

It will also prove necessary to consider the asymmetric quadrature problem

$$I_a^b[f](t) = \int_a^b f(\omega)e^{it\omega} d\omega.$$

in which F is approximated closely by a Fourier series in a given interval $[a, b]$ that is not necessarily symmetric with respect to the origin, and allowing, additionally, for the possibility that F does not vanish smoothly outside $[a, b]$.

To solve this modified problem we utilize the change of variables

$$I_a^b[F](t_\ell) = \int_a^b F(\omega)e^{-i\omega t_\ell} d\omega = \delta e^{-it_\ell\gamma} \int_{-W}^W F(\gamma + \delta\omega)e^{-i\tau_\ell\omega} d\omega,$$

where $\delta = \frac{b-a}{2W}$, $\gamma = \frac{b+a}{2}$ and $\tau_\ell = \delta t_\ell$.

Let P be the period of a Fourier series developed for F over an interval containing $[a, b]$. If $F \in C_{per}([a, b])$ then one might take $P = b - a$ and use FFTs to straightforwardly evaluate the Fourier coefficients. Otherwise we resort to using Fourier continuation [33, 34] to produce a high-order convergent interpolation of f in the interval, with $P \neq b - a$. In the end we have the expansion

$$F(\gamma + \delta\omega) = \sum_{m=-N/2}^{N/2-1} c_m e^{i\frac{2\pi}{P}m\omega}$$

After defining $t_\ell = \ell\Delta t$, $\beta = \frac{\delta P}{2\pi}\Delta t$ we proceed as before:

$$\begin{aligned} I_a^b[F](t_\ell) &= \delta e^{-it_\ell\gamma} \sum_{m=-N/2}^{N/2-1} c_m \int_{-W}^W e^{-i\frac{2\pi}{P}(\beta\ell-m)\omega} d\omega \\ &= \delta e^{-it_\ell\alpha} \sum_{m=-N/2}^{N/2-1} c_m \frac{P}{\pi(\beta\ell-m)} \operatorname{sinc}\left(\pi\frac{2W}{P}(\beta\ell-m)\right), \end{aligned}$$

which yields the formula,

$$I_a^b[F](t_\ell) = \delta e^{-it_\ell\alpha} \sum_{m=-N/2}^{N/2-1} c_m b_{\beta\ell-m}, \quad \text{where } b_q := 2W \operatorname{sinc}\left(\frac{2W}{P}q\right). \quad (41)$$

These expressions are scaled convolution, since generically $\beta \neq 1$. Firstly, for Equation (40) if $\beta = 1$ then we are picking out the zeros of the sinc function and the fact we obtain zero is not surprising since we are integrating sinusoids over their full period. Secondly, we may want a coarse discretization in time, or simply a different one. The problem may demand fine sampling in frequency to accurately resolve the wave scattering, but due to the independence of our solution at various time points there is no need to use the same temporal discretization for distinct sampling periods (no discretization error is introduced by the choice of time sampling). The scaled convolution cannot be directly evaluated with FFTs using the product of the frequency domain signals \widehat{b}, \widehat{c} , as would typically be done with a classical convolution. Instead, following the approach of Nascov and Logofătu [32] we use the Fractional Fourier Transform to efficiently evaluate the convolution, as described in the following section.

5.2 Scaled discrete convolutions via FFT and Fractional-Fourier-transform acceleration

In this section we consider the evaluation of discrete scaled convolutions of the form

$$d_\ell = \sum_{m=-N/2}^{N/2-1} c_m b_{\beta m - \gamma \ell}, \quad \ell \in \{\ell_0, \ell_1, \dots, \ell_{L-1}\}$$

Note that c_m are Fourier coefficients and it's assumed that $c_m = 0$ for $m > N/2$. Following Nascov and Logofătu [32] we proceed as follows. We first zero-pad c to be at least length L and compute the γ -fractional Fourier transform [35]

$$C_p^{(\gamma)} = \sum_{n=-M/2}^{M/2-1} c_n e^{-i \frac{2\pi \gamma n p}{M}}$$

$$B_p = \sum_{m=-M/2}^{M/2-1} b_m e^{-i \frac{2\pi m p}{M}}$$

Using the convolution theorem, we can easily see then that for the central N values, and in particular the L values of interest, we have [32]:

$$d_\ell = \sum_{m=-N/2}^{N/2-1} c_m b_{\beta m - \gamma \ell} = \frac{1}{M} \sum_{p=-M/2}^{M/2-1} C_p^{(\gamma)} B_p e^{i \frac{2\pi \beta \ell p}{M}}$$

Note that this last sum is an inverse fractional Fourier transform of scale β , while the computation of $C_p^{(\gamma)}$ is a fractional Fourier transform of scale γ . These fractional Fourier transforms (FRFTs) are accelerated with FFT-based fractional Fourier transform algorithms, at an $\mathcal{O}(N \log N)$ cost as required, approximately, by four classical FFT of length M ; see [35].

5.3 Non-smooth $F(\omega)$: singular quadrature for 2D low frequency scattering

Here we consider the problem of evaluating equation (12) in the case $d = 2$ for small ω where, as is known (MacCamy [36] and Werner [37]), in two dimensions the frequency dependence of solutions to the Helmholtz equation at $\omega = 0$ is not smooth. For this reason we have a need for a special quadrature rule for the two-dimensional problem as $\omega \rightarrow 0^\pm$. (Use of special low-frequency algorithms is not necessary for $d = 3$, since, in this case, the ω -dependence of the solution is smooth for all real values of ω , given smooth ω -dependence of the incident field [38, 39].)

To design our quadrature rule in the non-smooth case we first decompose the Fourier integral in the form

$$F(t_\ell) = \left(\int_{-W}^{-w_c} + \int_{-w_c}^{w_c} + \int_{w_c}^W \right) f(\omega) e^{-i\omega t} d\omega =: I_1 + I_0 + I_2$$

It then follows that

$$I_1 = I_{-W}^{-w_c}[f](t_\ell)$$

$$I_2 = I_{w_c}^W[f](t_\ell),$$

each of which can be treated with the Fourier-based quadrature developed in Section 5.1. Since $f = f(\omega)$ may not vanish as a function of ω at $\omega = \omega_c$, we utilize Fourier continuation [33, 34] to

retain a high-order convergent quadrature rule. However, an application of this approach to I_0 does not give rise to high-order accuracy, since, in the present non-smooth case, the resulting truncated Fourier series converges slowly. Instead, we develop a special quadrature rule for evaluation of the half-interval integral

$$I[f](t) = \int_0^{\omega_c} f(\omega) e^{-it\omega} d\omega \quad (42)$$

that retains the attractive features of our overall method.

In order to evaluate the solution at advanced time without growing cost due to the increasing oscillatory behavior of the transform kernel, we rely on the Filon-Clenshaw-Curtis-based quadrature approach [40]. The *classical* Filon-Clenshaw-Curtis method [41] involves replacement of the function $f(\omega)$ by its polynomial interpolant $Q_N f$ at the Clenshaw-Curtis points and computation of the resulting associated modified moments (which are given by integrals of the Chebyshev polynomials multiplied by the oscillatory Fourier kernel) exactly. This eliminates the need to interpolate the target transform function at large numbers of frequency points as time increases. Further, as shown in [40] the error decreases as $t \rightarrow \infty$.

We thus obtain the rule

$$I[f](t) = \int_{-1}^1 (Q_N f)(\omega) e^{it\omega} d\omega = \sum_{n=0}^N \alpha_{n,N}(f) M_n(t),$$

where, $M_n(t) := \int_{-1}^1 T_n(\omega) e^{it\omega} d\omega$, and

$$\alpha_{n,N}(f) = \frac{2}{N} \sum_{j=0}^N \cos\left(\frac{jn\pi}{N}\right) f(s_{j,N}), \quad s_{j,N} = \cos\left(\frac{j\pi}{N}\right).$$

For non-smooth f the method employed here uses, near the location of non-smooth behavior, a graded mesh of the form

$$\Pi_{M,q} := \left\{ x_j := \left(\frac{j}{M}\right)^q : j = 0, 1, \dots, M \right\}, \quad (43)$$

on subintervals of which individual grids of Clenshaw-Curtis points are employed, and, then the quadrature rule is applied to the evaluation of $I_{x_j}^{x_{j+1}} [f](t)$. The final integral is thus approximated by the composite rule

$$I_a^b [f](t) = \sum_{j=2}^M I_{x_{j-1}}^{x_j} [f](t). \quad (44)$$

The error introduced by this quadrature rule, which does not grow with increasing time for a fixed set of quadrature rule parameters, is discussed extensively in [40], and is of course dependent on the strength of the singularity. Briefly, in our context the convergence order in N (with $q > N+1$) is determined by choice of rule parameters M . Letting N be the number of Clenshaw-Curtis points per subinterval, and I_N be the result of this composite quadrature rule, we find the error in this quadrature rule to be [40, Thm. 3.6]

$$|I[f] - I_N[f]| = \mathcal{O}(M^{-(1+N)})$$

In this paper we choose in particular $M = 4$, $N = 8$, and $q = 9.1$. This error is only present in a two-dimensional context where the frequencies to be considered include an interval containing $\omega = 0$; for problems involving frequency spectrum bounded away from the origin, this use of this rule is not required. The computational cost of this algorithm does not grow with increasing evaluation time t , consistent with the claimed $\mathcal{O}(1)$ large time sampling cost.

6 Numerical Results

After a brief demonstration of the proposed quadrature rule in a simple context (Section 6.1), this section demonstrates the convergence of the overall algorithm (Section 6.2) and it presents solutions produced by the solver in the two-dimensional context (Subsections 6.3, and, for long-time multiple-scattering 6.4). Additionally, this section provides long-time demonstrations enabled by the time-partitioning methodology described in Section 4, including, in Section 6.4, cases in which very significant multiple scattering takes place.

6.1 Fourier Quadrature Demonstration

Figure 3 presents results for the algorithm described in section 5.1 for evaluation of Fourier integrals. We numerically compute the inverse Fourier transform of $f(w) = e^{-\frac{1}{4}w^2} e^{i3w}$ with a well-refined trapezoidal rule. With a simple change of sign of one of the parameters we can also compute the forward Fourier Transform (in the panel (c) of this figure we use as input the corresponding pair from the previous test.) Panels (d-e) show results using Fourier Continuation to expand the integrand in a Fourier series, as may be needed for aperiodic functions. For the forward transform the discretization h corresponds to the time sampling rate, while for the inverse transform the discretization h corresponds to the frequency spacing. High-order convergence of the quadrature method means the method is efficient in the number of expensive Helmholtz solves which are needed.

6.2 Convergence of solution

Since complex scattering problems do not generally have known exact solutions we show convergence tables relative to a fully-resolved solution obtained with our algorithm. The incident field $u^{inc}(\mathbf{r}, t)$ is given by its frequency-domain prescription:

$$U^{inc}(\mathbf{r}, \omega) = e^{-\frac{(\omega-\omega_0)^2}{\sigma^2}} e^{i\omega \frac{\mathbf{k}}{\|\mathbf{k}\|} \cdot \mathbf{r}}$$

where parameters used are $\omega_0 = 12, \sigma = 2, \mathbf{k} = \mathbf{e}_x + \frac{1}{2}\mathbf{e}_y$. The time trace of the scattered field at an observation point can be seen in Figure 4a, and the solution snapshot (albeit for a different value of ω_0) in Figure 5. The convergence analysis itself, in Figure 4b shows the superalgebraic convergence nature of the algorithm to the correct solution. In particular, significantly higher accuracy is reported here than elsewhere in the literature for similar problems.

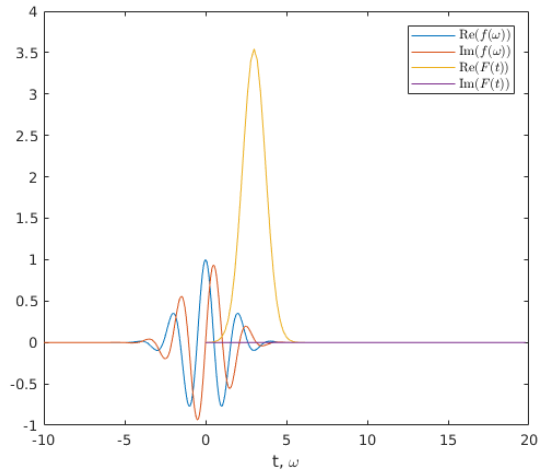
6.3 Full solver demonstration

This section presents results produced by the proposed methodology for a two-dimensional kite-shaped scatterer in the $d = 2$ case, the boundary of which acts as a sound-soft scatterer in the exterior. Figure 5 presents the computed solution for an incident field given in frequency-domain by a Gaussian-modulated plane wave

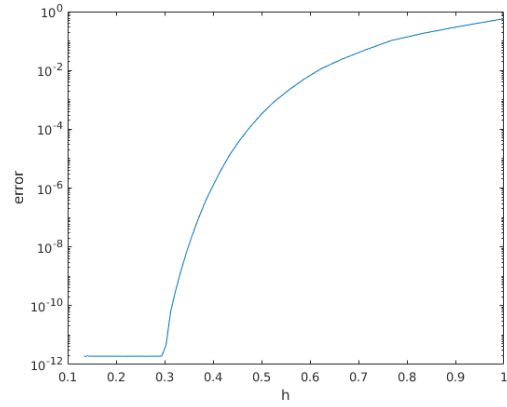
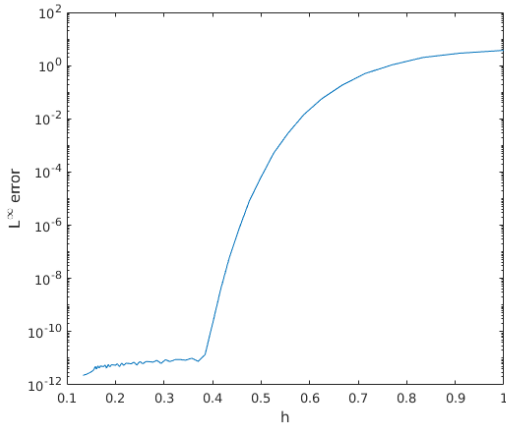
$$U^{inc}(\mathbf{r}, \omega) = e^{-\frac{(\omega-\omega_0)^2}{\sigma^2}} e^{i\omega \frac{\mathbf{k}}{\|\mathbf{k}\|} \cdot \mathbf{r}}$$

where parameters used are $\omega_0 = 8, \sigma = 2, \mathbf{k} = \mathbf{e}_x + \frac{1}{2}\mathbf{e}_y$.

To demonstrate the capability of the solver to handle a variety of incident fields, including those prescribed only in time-domain and with possibly long wave trains, Figure 7 shows a more

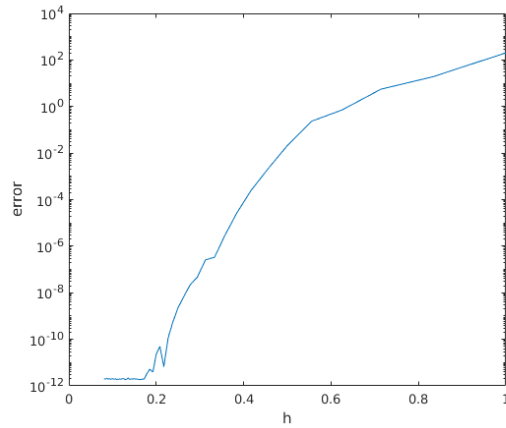
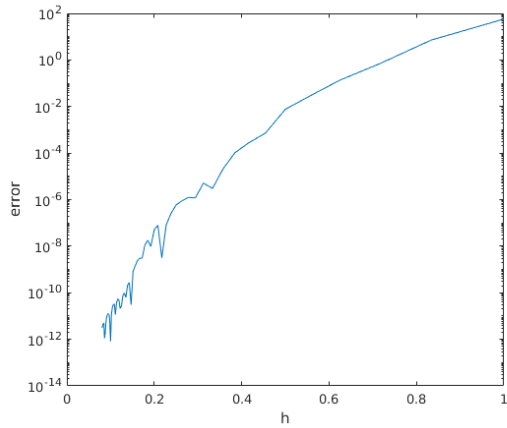


(a) Test function $f(\omega)$ and its inverse Fourier Transform.



(b) FRFT-accelerated (inverse) Fourier quadrature method.

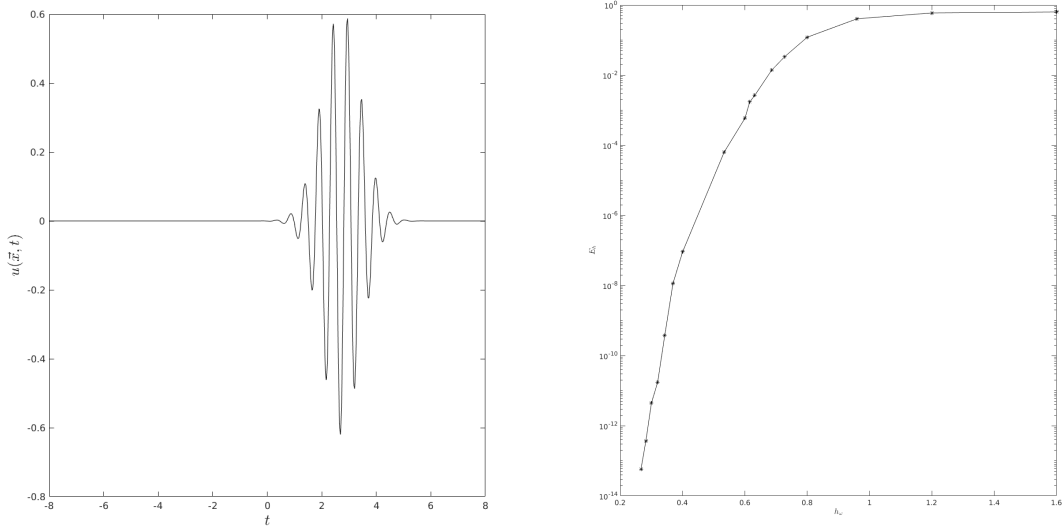
(c) FRFT-accelerated (forward) Fourier quadrature method.



(d) FRFT-accelerated (inverse) FC-Fourier quadrature method,

(e) FRFT-accelerated (forward) FC-Fourier quadrature method.

Figure 3: Convergence of accelerated Fourier quadrature methods.



(a) Time trace of the scattered field at the point (2, 2), exterior to the domain. (b) Maximum all-time error at (2, 2) as a function of the frequency-domain discretization h_ω .

Figure 4: Error in the overall solver for the problem for the problem considered in Section 6.2.

complicated set of time-dependent boundary conditions. The incident field is a plane wave directed at the rear of the kite-shaped scatterer, with amplitude following a linear chirp function; in detail,

$$\begin{aligned}
 g(t) &= 4t + 6 \cos\left(\frac{t}{\sqrt{12}}\right) \\
 f(t) &= \sin(g(t)) + \frac{1}{4000}g^2(t) \\
 u^{inc}(\mathbf{r}, t) &= f(t - \mathbf{r} \cdot \hat{\mathbf{k}}_{inc}).
 \end{aligned} \tag{45}$$

Due to the long duration of incidence the smooth time partitioning method described in Section 4.2 was used to produce these solutions. The solver relies on 200 frequency domain solutions and the near field solutions are plotted on a 128×128 grid.

We also demonstrate in Figure 6 the capabilities of the time window partitioning in conjunction with the active window tracking presented in Section 4; the incident field is again as prescribed in (45), though with a different angle of incidence $\hat{\mathbf{k}}$. In each of the four large panels (a)-(d), the top-left subfigure presents the total field, the overall solution $u^{tot}(\mathbf{r}, t)$. The remaining subfigures show the solution contribution from the individual time partitions (if the scattered field due to this window is determined not to contribute at a particular time for this evaluation region, the geometry is not plotted). Clearly not all partitions contribute at all times, and reliance on this fact can significantly accelerate computation of solution fields over long times.

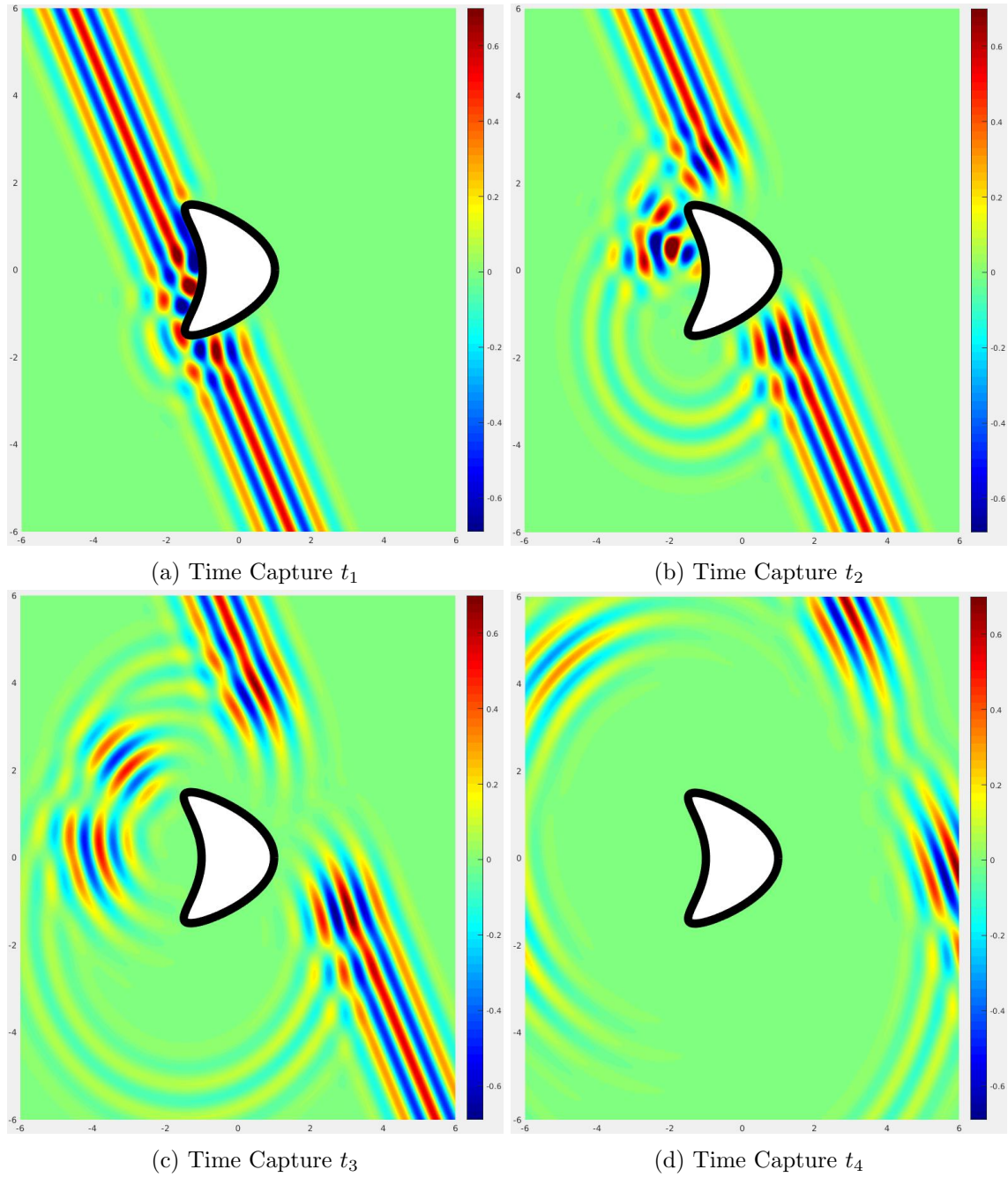
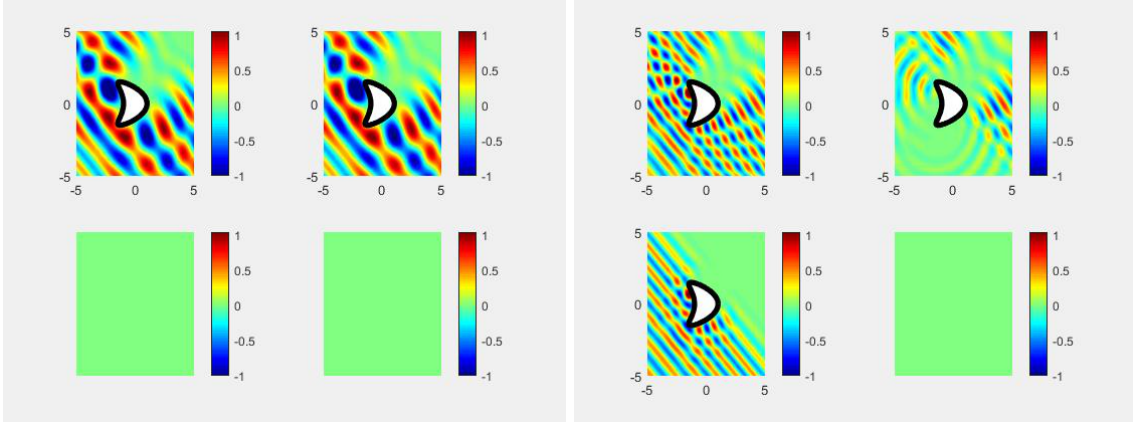
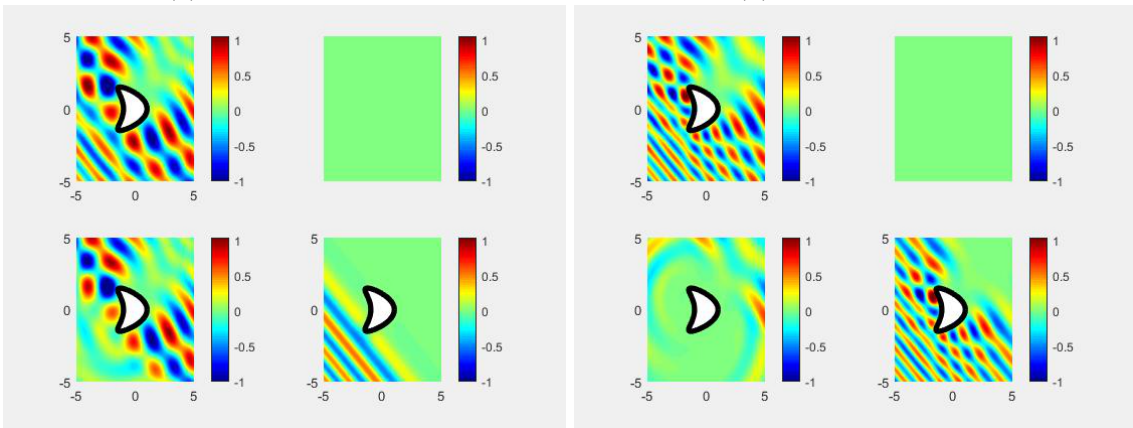


Figure 5: Total field produced by the proposed algorithm for the Gaussian-incidence problem described in Section 6.3.



(a) Time Capture t_1

(b) Time Capture t_2



(c) Time Capture t_3

(d) Time Capture t_4

Figure 6: Active-windows tracking demonstration described in Section 6.3.

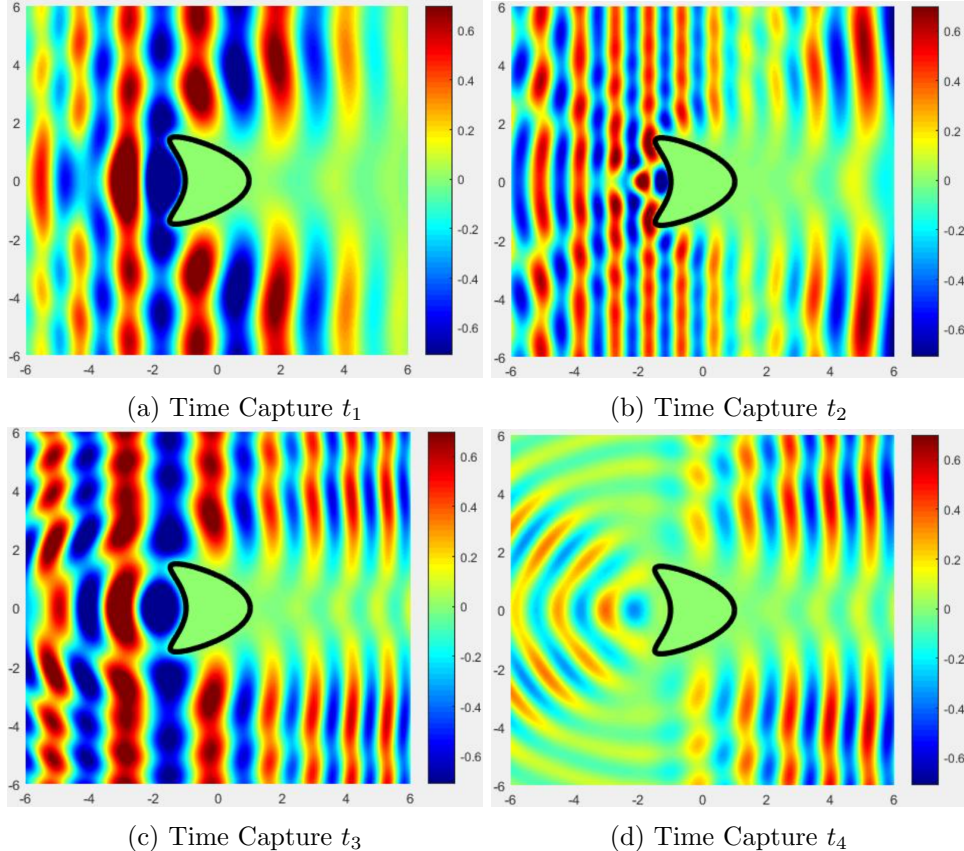


Figure 7: Total field produced by the smooth incident-field time-partitioning algorithm.

6.4 Long-time multiple scattering in “whispering gallery” geometry

In order to demonstrate the ability of the proposed method to evaluate solutions for long times we consider an incident wave impinging on a “whispering gallery” geometry, as depicted in Figure 8. This figure also displays solution snapshots at a variety of representative times. Notice that there is significant multiple scattering over the range of evaluation times. Highly accurate computation of this multiple-scattering solution over the long simulation interval, with all-time errors comparable to the errors inherent in the frequency-domain solutions, is enabled by the dispersionless properties of our algorithm.

7 Conclusion

This paper presents the first general algorithm with theoretically and experimentally-observed superalgebraically spectral convergence in both space and time for the solution of the time domain wave equation in two- and three-dimensional space. The overall hybrid frequency/time method runs in $\mathcal{O}(N)$ operations for evaluation of the solution at N points in time. Additionally, this is the first algorithm capable to produce arbitrarily-large time evaluation of scattered fields with $\mathcal{O}(1)$ cost. The method is embarrassingly parallelizable in time, and it is amenable to implementations involving a variety of acceleration techniques based on high performance computing.

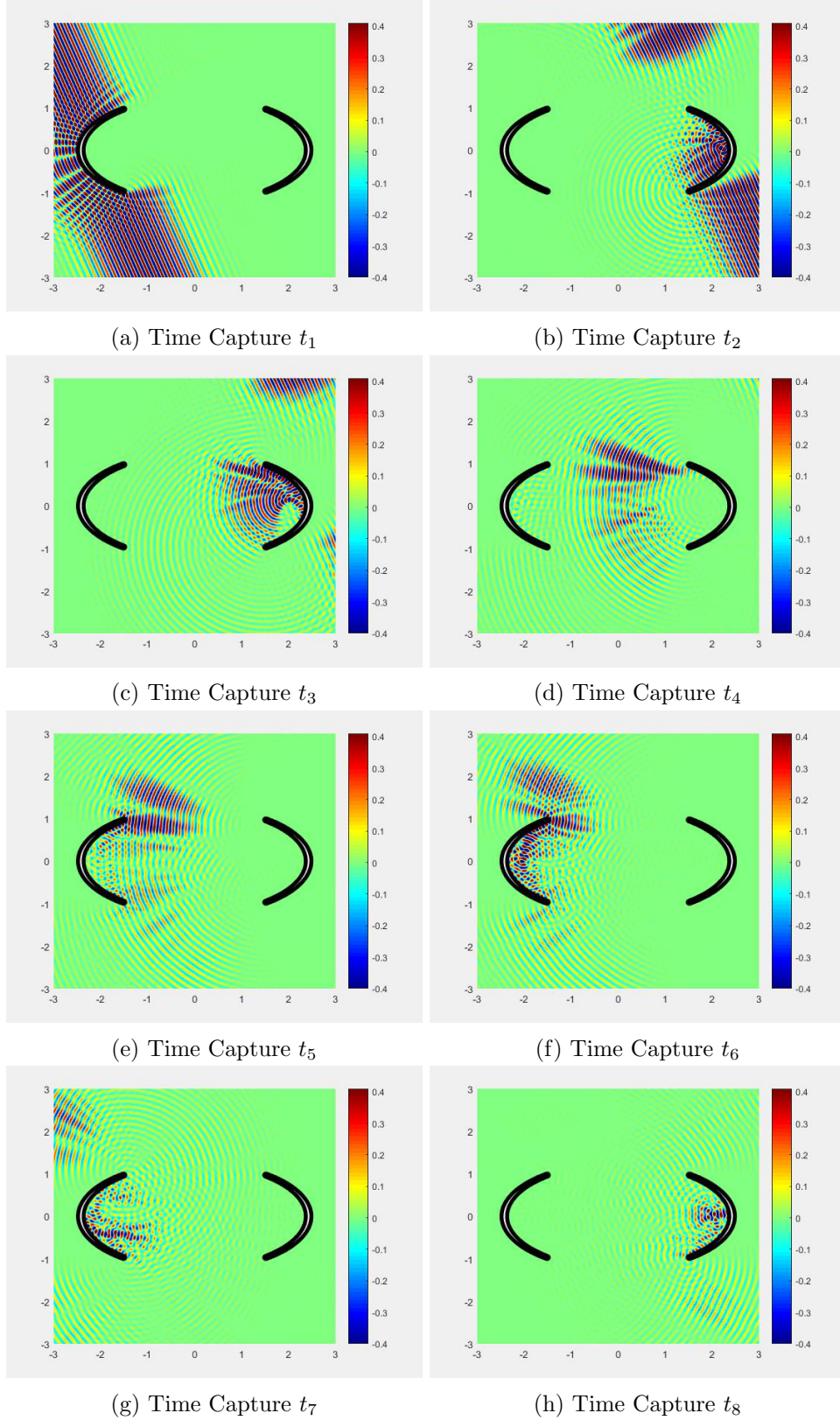


Figure 8: Total fields in the “Whispering Gallery” experiment described in Section 6.4. Note the multiple reflections that take place at the elliptical surfaces, over long propagation times and a significant number of scattering events.

Acknowledgements

The authors gratefully acknowledge support by NSF, AFOSR and DARPA through contracts DMS-1411876 and FA9550-15-1-0043 and HR00111720035, and the NSSEFF Vannevar Bush Fellowship under contract number N00014-16-1-2808. T. G. Anderson acknowledges support from the DOE Computational Sciences Fellowship, DOE grant DE-FG02-97ER25308.

References

- [1] A. Taflove. *Computational electrodynamics : the finite-difference time-domain method*. Boston: Artech House, 2000. ISBN: 1-58053-076-1.
- [2] J.-F. Lee, R. Lee, and A. Cangellaris. “Time-domain finite-element methods”. *IEEE Transactions on Antennas and Propagation* 45.3 (Mar. 1997), pp. 430–442.
- [3] A. B. et T. Ha Duong and J. C. Nedelec. “Formulation variationnelle espace-temps pour le calcul par potentiel retardé de la diffraction d’une onde acoustique (I)”. *Mathematical Methods in the Applied Sciences* 8.1 (1986), pp. 405–435.
- [4] T. Ha-Duong. “On Retarded Potential Boundary Integral Equations and their Discretisation”. *Topics in Computational Wave Propagation: Direct and Inverse Problems*. Ed. by M. Ainsworth, P. Davies, D. Duncan, B. Rynne, and P. Martin. Berlin, Heidelberg: Springer Berlin Heidelberg, 2003, pp. 301–336. ISBN: 978-3-642-55483-4.
- [5] A. Yilmaz, J.-M. Jin, and E. Michielssen. “Time Domain Adaptive Integral Method for Surface Integral Equations”. *IEEE Transactions on Antennas and Propagation* 52.10 (Oct. 2004), pp. 2692–2708.
- [6] C. L. Epstein, L. Greengard, and T. Hagstrom. *On the stability of time-domain integral equations for acoustic wave propagation*. 2015.
- [7] S. Petropavlovsky, S. Tsynkov, and E. Turkel. “A method of boundary equations for unsteady hyperbolic problems in 3D”. *Journal of Computational Physics* 365 (July 2018), pp. 294–323.
- [8] C. Lubich. “On the multistep time discretization of linear initial-boundary value problems and their boundary integral equations”. *Numerische Mathematik* 67.3 (Apr. 1994), pp. 365–389. ISSN: 0945-3245.
- [9] L. Banjai and S. Sauter. “Rapid Solution of the Wave Equation in Unbounded Domains”. *SIAM Journal on Numerical Analysis* 47.1 (2009), pp. 227–249.
- [10] L. Banjai. “Multistep and Multistage Convolution Quadrature for the Wave Equation: Algorithms and Experiments”. *SIAM Journal on Scientific Computing* 32.5 (2010), pp. 2964–2994.
- [11] L. Banjai and M. Schanz. “Wave Propagation Problems Treated with Convolution Quadrature and BEM”. *Fast Boundary Element Methods in Engineering and Industrial Applications*. Ed. by U. Langer, M. Schanz, O. Steinbach, and W. L. Wendland. Berlin, Heidelberg: Springer Berlin Heidelberg, 2012, pp. 145–184. ISBN: 978-3-642-25670-7.
- [12] L. Banjai and M. Kachanovska. “Fast convolution quadrature for the wave equation in three dimensions”. *Journal of Computational Physics* 279 (2014), pp. 103–126. ISSN: 0021-9991.
- [13] T. Betcke, N. Salles, and W. Śmigaj. “Overresolving in the Laplace Domain for Convolution Quadrature Methods”. *SIAM Journal on Scientific Computing* 39.1 (2017), A188–A213.

- [14] E. Mecocci, L. Misici, M. C. Recchioni, and F. Zirilli. “A new formalism for time-dependent wave scattering from a bounded obstacle”. *The Journal of the Acoustical Society of America* 107.4 (Apr. 2000), pp. 1825–1840.
- [15] M. C. Recchioni and F. Zirilli. “A new formalism for time-dependent electromagnetic scattering from a bounded obstacle”. *Journal of Engineering Mathematics* 47.1 (Sept. 2003), pp. 17–43. ISSN: 1573-2703.
- [16] T. Hagstrom and T. Warburton. “Complete radiation boundary conditions: minimizing the long time error growth of local methods”. *SIAM J. Numer. Anal.* 47 (2009), pp. 3678–3704.
- [17] J.-P. Berenger. “A perfectly matched layer for the absorption of electromagnetic waves”. *Journal of Computational Physics* 114.2 (Oct. 1994), pp. 185–200.
- [18] B. Engquist and A. Majda. “Absorbing boundary conditions for the numerical simulation of waves”. *Mathematics of Computation* 31.139 (Sept. 1977), pp. 629–629.
- [19] A. Bayliss and E. Turkel. “Radiation boundary conditions for wave-like equations”. *Communications on Pure and Applied Mathematics* 33.6 (Nov. 1980), pp. 707–725.
- [20] I. M. Babuška and S. A. Sauter. “Is the Pollution Effect of the FEM Avoidable for the Helmholtz Equation Considering High Wave Numbers?” *SIAM Journal on Numerical Analysis* 34.6 (Dec. 1997), pp. 2392–2423.
- [21] O. P. Bruno and L. A. Kunyansky. “A Fast, High-Order Algorithm for the Solution of Surface Scattering Problems: Basic Implementation, Tests, and Applications”. *Journal of Computational Physics* 169.1 (May 2001), pp. 80–110.
- [22] O. P. Bruno and E. Garza. “A Chebyshev-based rectangular-polar integral solver for scattering by general geometries described by non-overlapping patches”. arXiv:1807.01813 [math.NA] (2018).
- [23] Q. Chen, P. Monk, X. Wang, and D. Weile. “Analysis of Convolution Quadrature Applied to the Time-Domain Electric Field Integral Equation”. *Communications in Computational Physics* 11.2 (2012), pp. 383–399.
- [24] F.-J. Sayas. *Retarded Potentials and Time Domain Boundary Integral Equations*. Springer International Publishing, 2016.
- [25] O. P. Bruno, C. A. Geuzaine, J. A. Monro, and F. Reitich. “Prescribed error tolerances within fixed computational times for scattering problems of arbitrarily high frequency: the convex case”. *Philosophical Transactions of the Royal Society of London A: Mathematical, Physical and Engineering Sciences* 362.1816 (2004), pp. 629–645. ISSN: 1364-503X.
- [26] R. Kress. *Linear Integral Equations*. New York: Springer, 1999.
- [27] J. Stratton. *Electromagnetic theory*. New York, N.Y. Chicago, Ill: McGraw-Hill Book Company Adams Press distributor, 1941. ISBN: 1443730548.
- [28] N. N. Lebedev. *Special Functions & Their Applications*. Dover Publications, 1972. ISBN: 0486606244.
- [29] B. Baker and E. Copson. *The Mathematical Theory of Huygens’ Principle*. Oxford: Clarendon Press, 1950.
- [30] L. Felsen and N. Marcuvitz. *Radiation and scattering of waves*. New York: Prentice-Hall, 1973.

- [31] K. E. Atkinson. *The Numerical Solution of Integral Equations of the Second Kind (Cambridge Monographs on Applied and Computational Mathematics)*. Cambridge University Press, 2009. ISBN: 0521102839.
- [32] V. Nascov and P. C. Logofătu. “Fast computation algorithm for the Rayleigh-Sommerfeld diffraction formula using a type of scaled convolution”. *Appl. Opt.* 48.22 (Aug. 2009), pp. 4310–4319.
- [33] O. P. Bruno and M. Lyon. “High-order unconditionally stable FC-AD solvers for general smooth domains I. Basic elements”. *Journal of Computational Physics* 229.6 (Mar. 2010), pp. 2009–2033.
- [34] F. Amlani and O. P. Bruno. “An FC-based spectral solver for elastodynamic problems in general three-dimensional domains”. *Journal of Computational Physics* 307 (Feb. 2016), pp. 333–354.
- [35] D. H. Bailey and P. N. Swarztrauber. “The Fractional Fourier Transform and Applications”. *SIAM Review* 33.3 (1991), pp. 389–404.
- [36] R. C. MacCamy. “Low Frequency Acoustic Oscillations”. *Quarterly of Applied Mathematics* 23.3 (1965), pp. 247–255. ISSN: 0033569X, 15524485.
- [37] P. Werner. “Low frequency asymptotics for the reduced wave equation in two-dimensional exterior spaces”. *Mathematical Methods in the Applied Sciences* 8.1 (), pp. 134–156.
- [38] P. Werner. “Randwertprobleme der mathematischen Akustik”. *Archive for Rational Mechanics and Analysis* 10.1 (1962), pp. 29–66.
- [39] R. Kress. “On the limiting behaviour of solutions to boundary integral equations associated with time harmonic wave equations for small frequencies”. *Mathematical Methods in the Applied Sciences* 1.1 (1979), pp. 89–100.
- [40] V. Domínguez, I. G. Graham, and T. Kim. “Filon–Clenshaw–Curtis Rules for Highly Oscillatory Integrals with Algebraic Singularities and Stationary Points”. *SIAM Journal on Numerical Analysis* 51.3 (2013), pp. 1542–1566.
- [41] I. H. Sloan and W. E. Smith. “Product integration with the Clenshaw-Curtis points: Implementation and error estimates”. *Numerische Mathematik* 34.4 (Dec. 1980), pp. 387–401.